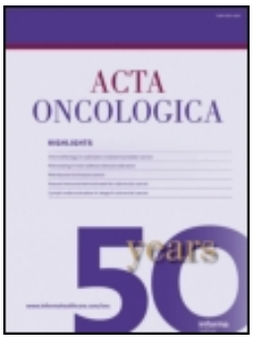

Acta Oncologica

ISSN: 0284-186X (Print) 1651-226X (Online) Journal homepage: informahealthcare.com/journals/ionc20

# Inter- and intrafractional localisation errors in cone-beam CT guided stereotactic radiation therapy of tumours in the liver and lung

Esben S. Worm, Anders T. Hansen, Jørgen B. Petersen, Ludvig P. Muren, Lars H. Præstegaard & Morten Høyer

**To cite this article:** Esben S. Worm, Anders T. Hansen, Jørgen B. Petersen, Ludvig P. Muren, Lars H. Præstegaard & Morten Høyer (2010) Inter- and intrafractional localisation errors in cone-beam CT guided stereotactic radiation therapy of tumours in the liver and lung, Acta Oncologica, 49:7, 1177-1183, DOI: 10.3109/0284186X.2010.498435

**To link to this article:** https://doi.org/10.3109/0284186X.2010.498435

*Acta Oncologica*, 2010; 49: 1177–1183

informa
healthcare

**ORIGINAL ARTICLE**

# Inter- and intrafractional localisation errors in cone-beam CT guided stereotactic radiation therapy of tumours in the liver and lung

ESBEN S. WORM[1], ANDERS T. HANSEN[1], JØRGEN B. PETERSEN[1], LUDVIG P. MUREN[1], LARS H. PRÆSTEGAARD[1] & MORTEN HØYER[2]

[1]*Department of Medical Physics, Aarhus University Hospital, Aarhus, Denmark and* [2]*Department of Oncology, Aarhus University Hospital, Aarhus, Denmark*

**Abstract**

*Background.* Localisation errors in cone-beam CT (CBCT) guided stereotactic body radiation therapy (SBRT) were evaluated and compared to positioning using the external coordinates of a stereotactic body frame (SBF) alone. Possible correlations to patient- or treatment-specific factors such as body mass index (BMI), planning time, treatment delivery time, and distance between tumour and spinal cord were explored to determine whether they influenced on the benefit of image-guidance. *Material and methods.* A total of 34 patients received SBRT (3 fractions) for tumours in the liver (15 patients) or the lung (19 patients). Immobilisation and positioning was obtained with a SBF. Pre- and post-treatment CBCT scans were registered with the bony anatomy of the planning CT to find inter- and intrafractional patient positioning errors (PPE). For lung tumour patients, matching was also performed on the tumours to find the tumour positioning errors (TPE) and baseline shifts relative to bony anatomy. *Results.* The mean inter- and intrafractional 3D vector PPE was 4.5 ± 2.7 mm (average ± SD) and 1.5 ± 0.6 mm, respectively, for the combined group of patients. For lung tumours, the interfractional misalignment was 5.6 ± 1.8 mm. The baseline shift was 3.9 ± 2.0 mm. Intrafractional TPE and baseline shifts were 2.1 ± 0.7 mm and 1.9 ± 0.6 mm, respectively. The magnitude of interfractional baseline shift was closely correlated with the distance between the tumour and the spinal cord. Intrafractional errors were independent of patient BMI, age or gender. *Conclusion.* Image-guidance reduced setup errors considerably. The study demonstrated the benefit of CBCT-guidance regardless of patient specific factors such as BMI, age or gender. Protection of the spinal cord was facilitated by the correlation between the tumour position relative to the spinal cord and the magnitude of baseline shift.

During the last decade hypofractionated extracranial stereotactic body radiation therapy (SBRT), in which a high total dose is given in a few treatment fractions, has proven to be an effective treatment option for targets such as small tumours in the lung and liver [1,2]. Because of the potential toxicity related to this escalated dose regime, accurate treatment planning and delivery is required for successful SBRT [3].

Conventionally, to achieve the demanded precision, a stereotactic body frame (SBF) has been used to define the reference system for target positioning [4]. A premise for precise treatment using this technique is that the patient can be repositioned accurately in the SBF. For overweight patients this is challenged by more variable internal/external anatomy. For example, position markers on the patient surface may be less reliable due to increased mobility with respect to bony anatomy [5,6]. Data in the literature describing relations between body habitus and setup errors in SBRT are very limited. One study found a significant correlation between loss of target volume coverage and body mass index (BMI)$>30$ in SBRT of lung and liver tumours using the BodyFIX double-vacuum system (Medical Intelligence, Schwabmünchen, Germany) for immobilisation [7]. Another group reported a significant relationship between the mobility of the diaphragm and BMI in male patients treated with SBRT for tumours in the liver [8].

The recent introduction of kilovoltage cone-beam CT (kV CBCT), with the ability to visualise target position before treatment, has potential of improving

Correspondence: Esben S. Worm, Department of Medical Physics, Aarhus University Hospital, Nørrebrogade 44, Building 5, 2nd floor, 8000 Aarhus C, Denmark. Tel: +45 8949 4464. Fax: +45 8949 4522. E-mail: esbeworm@rm.dk.

*(Received 19 May 2010; accepted 27 May 2010)*

ISSN 0284-186X print/ISSN 1651-226X online © 2010 Informa Healthcare
DOI: 10.3109/0284186X.2010.498435

the precision of dose delivery in SBRT [9]. An important feature is the possibility to correct for shifts of the tumour position relative to bony anatomy (baseline shifts) just prior to treatment. Several studies reported on reduction of setup errors using such techniques [10–16]. Baseline corrections do impose a risk of overdosing critical normal tissues like the spinal cord. To prevent this, a planning organ at risk volume (PRV) is often formed as a safety margin around critical organs [17]. However, in situations where the target is close to the organ at risk a large PRV volume can compromise target coverage.

In the present study, localisation errors in SBRT are investigated by comparing patient positioning using only SBF coordinates with positioning guided by CBCT. This information is used to examine whether patient BMI influence on the benefit of image-guidance and to test the feasibility of the PRV approach to protect the spinal cord. In addition, possible relations between setup errors and factors such as patient gender, age, planning time, and treatment delivery time are explored.

## Material and methods

The study includes 15 patients who received SBRT for either cholangiocarcinomas (n = 5), or metastases (n=10) in the liver and 19 patients who received SBRT for either non-small-cell lung cancer stage I (n = 9), stage II (n = 1), or lung metastases (n = 9). This cohort of patients comprises all patients treated in the period from October 2008 to October 2009 for which a full CBCT data set was obtained following our standard SBRT protocol. A single full CBCT data set, including a CBCT before and after each treatment fraction, was acquired for all lung tumour patients, corresponding to one isocentre/tumour in each patient. One of the liver tumour patients was treated using two individual isocentres (double CBCT data set, one for each of two metastases). A stereotactic body frame (SBF; Elekta Oncology Systems, Crawley, UK) was used for immobilisation in combination with abdominal compression. Four lung tumour patients and three liver tumour patients did not tolerate the abdominal compression and were immobilised with the SBF alone. Treatment planning was performed in Eclipse (Varian Medical Systems, Palo Alto, CA, USA), based on a 3 mm slice thickness helical planning CT scan (Brilliance Big Bore, Phillips Medical Systems, Bothell, WA, USA), using five to seven conformal treatment fields. The planning CT was acquired during free shallow breathing and intravenous contrast was applied to enhance the visibility of liver tumours. The planning target volume (PTV) was a 5-mm radial and 10-mm cranial-caudal expansion of the clinical target volume (CTV). The prescription dose to the CTV was 67.5 Gy to tumours in the lung and 45 Gy to tumours in the liver, delivered under free shallow breathing in three fractions. A PRV margin of 10 mm was applied to protect the oesophagus and spinal cord with dose constraints of maximum 7 Gy and 6 Gy per fraction, respectively. In cases where the PRVs compromised target coverage, the PRV was reduced together with the allowed magnitude of baseline shift correction at the treatment.

All patients were positioned using the external stereotactic coordinate system of the SBF. Before treatment, a 3-mm slice thickness kV CBCT (On-Board Imager; Varian Medical Systems) was acquired to evaluate and correct for interfractional localisation errors (liver patients: 125 kV CBCT and 1.8 cGy per scan, lung tumour patients: 110 kV CBCT and 0.5 cGy per scan). All CBCT scans were acquired using a full 360-degree rotation with an acquisition time of approximately 60 s. For patients treated for liver tumours, a soft tissue match on the tumour was unfeasible due to poor image contrast between tumour and liver tissue. Bony anatomy (vertebral spine on the level of the lesion) was used as tumour surrogate and auto-registered with the planning CT in our on-line image-guidance software (On-Board Imager application, version 1.4; Varian Medical Systems). Misalignment of bony anatomy was defined as the patient positioning error (PPE). For patients treated for lung tumours, automatic soft tissue co-registration (mutual gray value) between the CBCT and the planning CT was performed, using a region of interest in the match defined as the gross tumour volume delineated on the planning CT with a 1 cm isotropic margin. The result of this match defined the tumour positioning error (TPE). The baseline shift was found as the difference between the match on the tumour and a match using bony anatomy. All image registrations were validated by a radiation therapist and a medical physicist before treatment. An approach of using only the three translatory degrees of freedom (DOF) in the image registrations, thereby neglecting rotations, was chosen to enforce a matching result that could be corrected by the couch, which could not realise rotational corrections. For example, using a six DOF matching as an alternative on a patient with rotational misalignment only would have resulted in a translatory shift result of zero, even though translations alone could improve the tumour-alignment as well.

Analysis of patient and tumour positioning was performed following the margin recipe developed by van Herk et al. [18]. In short, the population group mean (GM), systematic errors ($\Sigma$), and random errors ($\sigma$) were calculated in the three orthogonal directions left-right (LR), cranial-caudal (CC), and

anterior-posterior (AP). The value GM was defined as the average of all individual patient misalignments. Systematic errors were calculated as the standard deviation (SD) of the individual means, and random errors were the root–mean–square of the individual SDs. From these, the PTV margin ($M$) required to ensure dose coverage of the CTV for 90% of the population is given by:

$$M = 2.5\Sigma + \beta\sqrt{\sigma^2 + \sigma_p^2} - \beta\sigma_p \qquad (1)$$

where $\sigma_p$ is the gaussian width of the penumbra, and $\beta$ is the value of the inverse cumulative standard normal distribution at the prescribed PTV minimum dose level. Values of both 1.64 and 0.84 were used for $\beta$ corresponding to the 95% and 80% isodose level respectively; the latter is often used for prescription in SBRT. To estimate the margin in water equivalent material, $\sigma_p$ was set to 3.2 mm, and in the lung, where the penumbra is broader, a value of 6.4 mm was used for $\sigma_p$ [15]. The values of $\Sigma$ and $\sigma$ in Equation 1 were calculated as the quadratic sum of the inter- and intrafractional errors.

Upper statistical outliers were defined using an interquartile based method, where upper outliers were defined as values greater than the sum of the upper quartile of the data set and the interquartile range multiplied by a factor of 1.5 [19]. Correlation analysis was performed using Spearman's non-parametric regression, yielding the Spearman correlation coefficient $r_s$ and the two tailed p-value. (statistical software R, Development Core Team, 2009). Patient BMI was calculated as patient weight (kg) divided by the square height ($m^2$).

## Results

Due to the 60 s acquisition time some motion blurring effects, which were generally absent on the planning CT, were observed on the CBCT scans of the lung tumours, implying that the automatic registration algorithm had to match two slightly different-looking lung tumour volumes (see discussion). However, match validations did in general not lead to any manual corrections of the automatic image registrations, except for three patients; one with a very small tumour (diameter $<$ 6 mm), and two with a tumour located close to the diaphragm.

Combining all patients in one group, the average three-dimensional (3D) misalignment of bony anatomy was 4.5 $\pm$ 2.7 mm (mean $\pm$ SD vector length). Tables I and II summarise the interfractional errors for the two sub-groups of patients. The considerable difference in PPE of the two patient groups in the CC direction could be traced to the existence of two statistical upper outliers in the combined 3D vector PPE dataset (upper outlier fence = 10.6 mm), both lung tumour patients, with mean misalignment of bony anatomy of 11.0 mm and 13.4 mm, respectively. Without these outliers, the PPE's of the two patient groups (liver and lung) differed less than 0.4 mm. The outliers are included in all further analysis. For lung tumours, TPE and baseline shifts are also shown in Table II. The mean TPE was 5.6 $\pm$ 1.8 mm and baseline shift was 3.9 $\pm$ 2.0 mm. The absolute 3D tumour mismatch that would have been present at each treatment fraction if bony alignment had been used instead of tumour alignment are shown in Figure 1.

Intrafractional systematic and random PPE's were in the sub-mm range for both liver and lung patients. The mean shift of bony anatomy during treatment was 1.5 $\pm$ 0.6 mm. Similarly, for the

Table I. Inter- and intra-fraction PPE for the 15 patients treated for liver tumours.

| | LR (mm) | CC (mm) | AP (mm) |
|---|---|---|---|
| Interfraction PPE[1] | | | |
| GM | 0.9 | 0.3 | 0.8 |
| $\Sigma$ | 1.9 | 2.7 | 1.3 |
| $\sigma$ | 2.1 | 1.5 | 1.5 |
| Intrafraction PPE[1] | | | |
| GM | 0.2 | 0.2 | 0.2 |
| $\Sigma$ | 0.9 | 0.5 | 0.7 |
| $\sigma$ | 0.7 | 0.7 | 0.7 |

Abbreviations: LR = left-right, CC = cranial-caudal, AP = anterior-posterior, PPE = patient positioning error, GM = group mean, $\Sigma$ = systematic error, $\sigma$ = random error.
[1]Includes data from 16 individual isocentres. One of the patients was treated using two isocentres.

Table II. Interfraction alignment errors of bony anatomy, tumour, and baseline for the 19 patients treated for lung tumours.

| | LR (mm) | CC (mm) | AP (mm) |
|---|---|---|---|
| Bone (PPE) | | | |
| GM | 1.4 | 0.2 | 0.0 |
| $\Sigma$ | 2.3 | 4.5 | 1.6 |
| $\sigma$ | 1.9 | 2.8 | 1.4 |
| Tumour (TPE)[1] | | | |
| GM | 1.0 | 0.3 | 0.0 |
| $\Sigma$ | 2.5 | 3.8 | 2.8 |
| $\sigma$ | 1.7 | 2.7 | 2.1 |
| Baseline shift[1] | | | |
| GM | 0.3 | –0.4 | –0.2 |
| $\Sigma$ | 1.1 | 2.9 | 2.9 |
| $\sigma$ | 0.8 | 1.7 | 1.6 |

Abbreviations: LR = left-right, CC = cranial-caudal, AP = anterior-posterior, PPE = patient positioning error, TPE = tumour positioning error, GM = group mean, $\Sigma$ = systematic error, $\sigma$ = random error.
[1]Tumor and baseline data only includes 18 of the 19 lung tumours. In one of the patients the tumour was not identifiable on the CBCT.

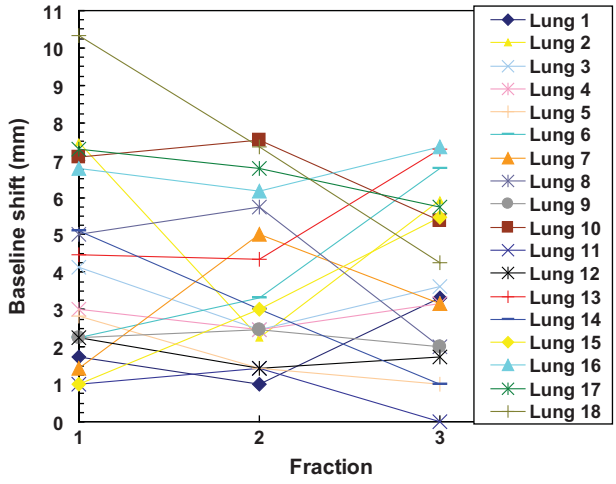


Figure 1. The magnitude of the interfractional baseline shift (3D) for each treatment fraction of the patients treated for lung tumours.

patients treated for lung tumours, both the intrafractional tumour and baseline errors were below 1 mm, except for the random errors in the CC and AP directions. Intrafractional errors for the two patient groups are summarised in Tables I and III. The intrafractional shift of the tumour position and the baseline shift were 2.1 ± 0.7 mm and 1.9 ± 0.6 mm, respectively.

Using tumour alignment as the ground truth, the PTV margins required to account for the determined localisation errors of the patients treated for lung tumours, are shown in Table IV. Conservatively, in the margin analysis intrafraction position changes were assumed to be present during the whole treatment. This approach was chosen because the errors also contain components from inaccuracies in table correction/position and CBCT to planning CT image registration. In addition, no correlation was found between treatment time and intrafractional TPE (see below).

Table III. Intrafraction alignment errors of bony anatomy, tumour, and baseline for the 19 patients treated for lung tumours.

| | LR (mm) | CC (mm) | AP (mm) |
|---|---|---|---|
| Bone (PPE) | | | |
| GM | 0.3 | 0.4 | 0.4 |
| Σ | 0.7 | 0.7 | 0.6 |
| σ | 0.9 | 1.0 | 0.8 |
| Tumour (TPE)[1] | | | |
| GM | 0.4 | 0.3 | 0.5 |
| Σ | 0.8 | 0.8 | 0.7 |
| σ | 0.8 | 1.7 | 1.1 |
| Baseline shift[1] | | | |
| GM | 0.0 | 0.0 | –0.1 |
| Σ | 0.7 | 0.7 | 0.6 |
| σ | 0.9 | 1.7 | 1.2 |

[1]Tumor and baseline data only includes 18 of the 19 lung tumours. In one of the patients the tumour was not identifiable on the CBCT.

The mean BMI of all patients (excluding four for which no BMI was recorded) was 24.9 ± 4.4. Figure 2 shows the significant correlation between patient BMI and mean interfraction 3D PPE of the three treatment fractions ($r_s$ = 0.44, p = 0.014) for all patients grouped together. However, when patients treated without abdominal compression (four of these patients were too large to fit into the SBF with compression) were removed from the data set, no significant correlation could be determined. No correlation was found between intrafractional 3D PPE and BMI (p = 0.51). For lung tumours, the magnitude of interfractional baselines shift was found to be closely related ($r_s$ = 0.74, p < 0.001) to the distance between tumour and spinal cord (Figure 3), with no statistical significant dependency on the use of abdominal compression or not. The distance was measured on the planning CT as the 2D distance from the centre of gravity of the CTV to the centre of the spinal cord in the CT-slice containing the isocenter. No intrafractional correlation was found.

The intrafractional 3D PPE's correlated weakly ($r_s$ = 0.35) but significant (p<0.001) with the time range between the pre- and post-treatment CBCT scans (23.6 ± 6.2 minutes). No significant correlation (p = 0.34) was found between intrafractional TPE of the lung tumours and treatment time. The time between planning CT and first treatment fraction was 10.1 ± 2.5 days for all patients and 10.2 ± 2.2 days for the sub-group of patients treated for lung tumours and did not correlate with either PPE of all patients (p = 0.39) or baseline shifts of the lung tumours (p = 0.58). No significant relations were found of either inter- or intrafractional PPE or tumour position with respect to patient age or gender.

## Discussion

CBCT-guidance combined with the SBF effectively reduced both the systematic and random PPE's to the sub-mm range compared to the few millimetres observed using the SBF alone. Similar findings were reported in other studies [10,12,20] performed using the CBCT system of an Elekta linear accelerator (Elekta Oncology Systems, Crawley, UK). Slightly larger intrafractional errors were found by Sonke et al. [15] using only arm and knee support for the patient during treatment. The presence of mean 3D misalignment of bony anatomy above 11 mm (two outliers) was reduced to a maximum intrafractional misalignment of 3.2 mm, using image-guidance. This is an important point since outliers have a high risk of target miss. Consequently,

Table IV. PTV margins required to account for the determined inter- and intra-fractional systematic and random localisation errors of the patients treated for lung tumors.

| | LR PTV (mm) | | | CC PTV (mm) | | | AP PTV (mm) | | |
|---|---|---|---|---|---|---|---|---|---|
| | Water (95%) | Lung (95%) | Lung (80%) | Water (95%) | Lung (95%) | Lung (80%) | Water (95%) | Lung (95%) | Lung (80%) |
| SBF alone | 7.3 | 6.9 | 6.7 | 12.0 | 11.0 | 10.4 | 8.6 | 8.0 | 7.6 |
| CBCT, Bones | 3.6 | 3.5 | 3.4 | 8.8 | 8.3 | 7.9 | 8.2 | 7.8 | 7.6 |
| CBCT, Tumour | 2.1 | 2.0 | 1.9 | 2.8 | 2.4 | 2.2 | 2.0 | 1.8 | 1.7 |

Abbreviations: LR = left-right, CC = cranial-caudal, AP = anterior-posterior
Margins are calculated according to Equation 1, assuming all tumours are surrounded by either water density-equivalent tissue or lung tissue. Margins ensuring dose coverage of the CTV with both the 95% and 80% dose level are stated using either SBF coordinates alone, CBCT match on bony anatomy, or CBCT match on the tumour for positioning.

CBCT-guidance not only improves the average accuracy but also helps to prevent such very critical positioning errors.

The substantial interfractional baseline changes found in this study have also previously been reported in the literature [10,11,15] and demonstrate the necessity of verifying tumour position before treatment. Without CBCT-guidance, large PTV margins of more than 10 mm were required (CC directions). Only a minor decrease of the margins was found using bony anatomy as a tumour surrogate. Applying soft-tissue image registration on the lung tumours substantially decreased margins to a level below 2.5 mm in all directions. The small intrafractional baseline shifts are in good agreement with the results reported from other groups [10,11,15]. It should be noted that the measured systematic errors will be larger than the underlying population systematic error distributions, because the random errors do not average out in only three treatment fractions. On the other hand, this implicitly accounts for the missing/limited blurring effect of the dose distribution that is assumed for random errors in the margin analysis [18]. Consequently, also in the case of few treatment fractions the statistical margin approach has been shown to provide reliable results [15].

A 10-mm isotropic PRV margin offered a good protection of normal tissue against baseline shifts (Figure 1). In cases where a PRV of this size compromised dose coverage of the tumour, a smaller margin was accepted. In no situations however, did the necessary baseline correction compromise the reduced PRV. This fact is related to the finding that baseline shifts increased with the distance from the spinal cord (Figure 3), thus facilitating the PRV approach. In addition, this demonstrates that image-guidance relying on bony anatomy becomes less accurate when the distance from the tumour to the

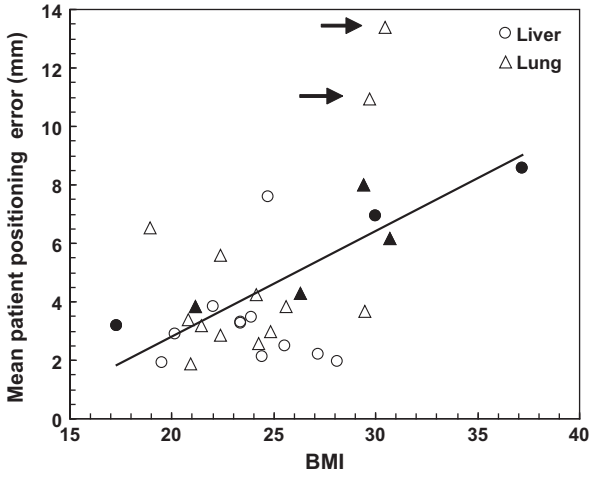


Figure 2. Interfraction mean PPE (3D) as a function of patient BMI. Patients treated without abdominal compression are marked with filled circles and triangles. Upper outliers are marked with arrows (upper fence = 10.6 mm). The correlation is significant when patients treated without compression are included ($r_s$ = 0.44, p = 0.014), but not if they are excluded from the data set ($r_s$ = 0.19, p = 0.37). A straight line is fitted to all of the data points (Pearson correlation coefficient r = 0.56).

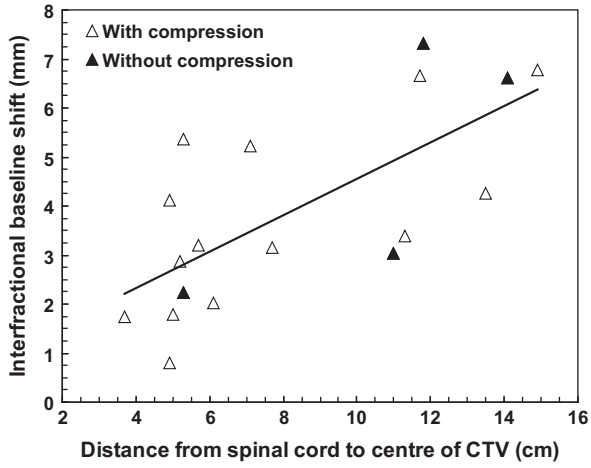


Figure 3. Mean interfractional baseline shift (3D) of the lung tumours as a function of the distance between the tumour and the spinal cord as measured on the planning CT ($r_s$ = 0.74, p < 0.001, including both patients treated with and without abdominal compression). A straight line is fitted to the all of the data points (Pearson correlation coefficient r = 0.70).

bony structures (vertebral spine) is large. The correlation between tumour-to-spinal cord distance and baseline shifts can be explained by the existence of more intervening tissue that can change or move from the time of acquisition of the planning CT to the time of treatment when the distance is large. Another contributing factor might be small rotational inaccuracies in patient positioning that could translate into a baseline shift, increasing with the distance to the spine, when performing only translatory matching and correction.

Due to the lack of soft tissue contrast, liver tumours are not distinguishable from the liver itself in CBCT images. To compensate for this, the dome of the diaphragm has been used as surrogate for the tumour position [13,14]. However, Wunderink et al. [21] recently found substantial discrepancies between setup based on liver-implanted fiducial markers, the diaphragm, and bony anatomy and concluded that diaphragm-based methods should be approached with care. To improve the general setup accuracy of such patients we are currently working on the implementation of CBCT-guidance using fiducial markers implanted in the liver.

It is not possible to determine whether the inaccuracy in positioning of large BMI patients was caused by the substantial fraction of these patients treated without abdominal compression (Figure 2). Nevertheless, the relationship shows that without IGRT, it is important to investigate and adapt the setup margins needed according to patient or treatment specific details such as BMI and the use of abdominal compression. Since no intrafractional BMI relationship was found, this study validates the effectiveness of CBCT-guidance to reduce setup errors, regardless of BMI or use of abdominal compression. In contrast to Purdie et al. [10] but in agreement with both Sonke et al. [15] and Guckenberger et al. [20], intrafraction TPE did not correlate with treatment time. However, the stability of bony anatomy did show weak, but significant, dependency on treatment time. Therefore, we recommend keeping treatment times as short as possible. The planning time did not seem to be important for setup accuracy within the short time range around ten days observed in this study.

The satisfactory auto-match results observed in the present study indicates that the motion induced effect of blurring of the CBCT scans in general was small enough to produce only minor difficulties for the matching algorithm when matching with the planning CT. Nevertheless, co-registration of images obtained under different conditions will introduce some uncertainties in both automatic and manual image matching that should be quantified. Errors arising from other sources like target delineation, uncertainty in table position, and respiratory tumour motion are also beyond the scope of this paper, but should all be determined locally and incorporated into Equation 1 or similar margin recipes. The recent introduction of advanced 4DCT imaging for both planning and image-guidance has shown improved potential of dealing with tumour motion in SBRT and to retain information that enables the quantification of clinically realistic PTV margins [15,22,23]. Treatment delivery at selected phases of the respiratory cycle (gating) sometimes aided by active breathing control (ABC) devices are well-known examples of other advanced methods used in the management of mobile tumours. However, these techniques mainly target errors due to random (respiratory) tumour motion, and not the far more critical systematic tumour positioning errors. Several recent studies confirmed the limited value of gating [24–27], at least without complimentary image-guidance. On this basis, CBCT-guidance is highly recommended as a first step for clinics considering ways of improving the accuracy in SBRT based on conventional positioning systems like the SBF.

In conclusion, CBCT-guided treatment is an effective way of minimising localisation errors in SBRT. CBCT-guidance in general more than halved the setup margins needed to ensure dose coverage of tumours in the lung compared to positioning based on SBF coordinates alone. In addition, this study demonstrated the value of CBCT-guidance regardless of patient specific factors such as BMI, age or gender. The evaluation of baseline shifts confirmed the necessity for soft tissue matching and such methods should be further investigated for use in SBRT of tumours in the liver. Finally, the PRV approach proved to be a straightforward way of handling the risk that baseline shifts imposes to key organs at risk.

## Acknowledgements

Supported by CIRRO – The Lundbeck Foundation Center for Interventional Research in Radiation Oncology and The Danish Council for Strategic Research.

***Declaration of interest:*** The authors report no conflicts of interest. The authors alone are responsible for the content and writing of the paper.

## References

[1] Rusthoven KE, Hammerman SF, Kavanagh BD, Birtwhistle MJ, Stares M, Camidge DR. Is there a role for consolidative stereotactic body radiation therapy following first-line systemic therapy for metastatic lung cancer? A patterns-of-failure analysis. Acta Oncol 2009;48:578–83.

[2] Martin A, Gaya A. Stereotactic body radiotherapy: A review. Clin Oncol (R Coll Radiol) 2010;22:157–72.
[3] Høyer M. Improved accuracy and outcome in radiotherapy of lung cancer. Radiother Oncol 2008;87:1–2.
[4] Blomgren H, Lax I, Näslund I, Svanström R. Stereotactic high dose fraction radiation therapy of extracranial tumors using an accelerator. Clinical experience of the first thirty-one patients. Acta Oncol 1995;34:861–70.
[5] Johansen J, Bertelsen A, Hansen CR, Westberg J, Hansen O, Brink C. Set-up errors in patients undergoing image guided radiation treatment. Relationship to body mass index and weight loss. Acta Oncol 2008;47:1454–58.
[6] Choi M, Fuller CD, Wang SJ, Siddiqi A, Wong A, Thomas CR, et al. Effect of body mass index on shifts in ultrasound-based image-guided intensity-modulated radiation therapy for abdominal malignancies. Radiother Oncol 2009;91:114–9.
[7] Fuss M, Salter BJ, Rassiah P, Cheek D, Cavanaugh SX, Herman TS. Repositioning accuracy of a commercially available double-vacuum whole body immobilization system for stereotactic body radiation therapy. Technol Cancer Res Treat 2004;3:59–67.
[8] Herfarth KK, Debus J, Lohr F, Bahner ML, Fritz P, Höss A, et al. Extracranial stereotactic radiation therapy: Set-up accuracy of patients treated for liver metastases. Int J Radiat Oncol Biol Phys 2000;46:329–35.
[9] Jaffray DA, Siewerdsen JH, Wong JW, Martinez AA. Flat-panel cone-beam computed tomography for image-guided radiation therapy. Int J Radiat Oncol Biol Phys 2002;53:1337–49.
[10] Purdie TG, Bissonnette JP, Franks K, Bezjak A, Payne D, Sie F, et al. Cone-beam computed tomography for on-line image guidance of lung stereotactic radiotherapy: Localization, verification, and intrafraction tumor position. Int J Radiat Oncol Biol Phys 2007;68:243–52.
[11] Guckenberger M, Meyer J, Wilbert J, Baier K, Mueller G, Wulf J, et al. Cone-beam CT based image-guidance for extracranial stereotactic radiotherapy of intrapulmonary tumors. Acta Oncol 2006;45:897–906.
[12] Grills IS, Hugo G, Kestin LL, Galerani AP, Chao KK, Wloch J, et al. Image-guided radiotherapy via daily online cone-beam CT substantially reduces margin requirements for stereotactic lung radiotherapy. Int J Radiat Oncol Biol Phys 2008;70:1045–56.
[13] Guckenberger M, Sweeney RA, Wilbert J, Krieger T, Richter A, Baier K, et al. Image-guided radiotherapy for liver cancer using respiratory-correlated computed tomography and cone-beam computed tomography. Int J Radiat Oncol Biol Phys 2008;71:297–304.
[14] Case RB, Sonke JJ, Moseley DJ, Kim J, Brock KK, Dawson LA. Inter- and intrafraction variability in liver position in non-breath-hold stereotactic body radiotherapy. Int J Radiat Oncol Biol Phys 2009;75:302–8.
[15] Sonke JJ, Rossi M, Wolthaus J, van Herk M, Damen E, Belderbos J. Frameless stereotactic body radiotherapy for lung cancer using four-dimensional cone beam CT guidance. Int J Radiat Oncol Biol Phys 2009;74:567–74.
[16] Masi L, Casamassima F, Menichelli C, Pasciuti K, Doro R, Polli C, et al. On-line image guidance for frameless stereotactic radiotherapy of lung malignancies by cone beam CT: Comparison between target localization and alignment on bony anatomy. Acta Oncol 2008;47:1422–31.
[17] International Commission on Radiation Units and Measurements. ICRU Report 62: Prescribing, recording and reporting photon beam therapy (supplement to ICRU report 50). Bethesda; ICRU: 1999.
[18] van Herk M, Remeijer P, Rasch C, Lebesque JV. The probability of correct target dosage: Dose-population histograms for deriving treatment margins in radiotherapy. Int J Radiat Oncol Biol Phys 2000;47:1121–35.
[19] Frigge M, Hoaglin DC, Iglewicz B. Some implementations of the Boxplot. Am Statist 1989;43:50–4.
[20] Guckenberger M, Meyer J, Wilbert J, Richter A, Baier K, Mueller G, et al. Intra-fractional uncertainties in cone-beam CT based image-guided radiotherapy (IGRT) of pulmonary tumors. Radiother Oncol 2007;83:57–64.
[21] Wunderink W, Romero AM, Seppenwoolde Y, de Boer H, Levendag P, Heijmen B. Potentials and limitations of guiding liver stereotactic body radiation therapy set-up on liver-implanted fiducial markers. Int J Radiat Oncol Biol Phys 2010 (in press).
[22] Ehler ED, Tomé WA. Lung 4D-IMRT treatment planning: An evaluation of three methods applied to four-dimensional data sets. Radiother Oncol 2008;88:319–25.
[23] Wang L, Hayes S, Paskalev K, Jin L, Buyyounouski MK, Ma CCM, et al. Dosimetric comparison of stereotactic body radiotherapy using 4D CT and multiphase CT images for treatment planning of lung cancer: Evaluation of the impact on daily dose coverage. Radiother Oncol 2009;91:314–24.
[24] Juhler-Nøttrup T, Korreman SS, Pedersen AN, Persson GF, Aarup LR, Nyström H, et al. Interfractional changes in tumour volume and position during entire radiotherapy courses for lung cancer with respiratory gating and image guidance. Acta Oncol 2008;47:1406–13.
[25] Korreman SS, Juhler-Nøttrup T, Persson GF, Pedersen AN, Enmark M, Nystrom H, et al. The role of image guidance in respiratory gated radiotherapy. Acta Oncol 2008;47: 1390–6.
[26] Muirhead R, Featherstone C, Duffton A, Moore K, McNee S. The potential clinical benefit of respiratory gated radiotherapy (RGRT) in non-small cell lung cancer (NSCLC). Radiother Oncol 2010;95:172–7.
[27] Guckenberger M, Krieger T, Richter A, Baier K, Wilbert J, Sweeney RA, et al. Potential of image-guidance, gating and real-time tracking to improve accuracy in pulmonary stereotactic body radiotherapy. Radiother Oncol 2009;91:288–95.